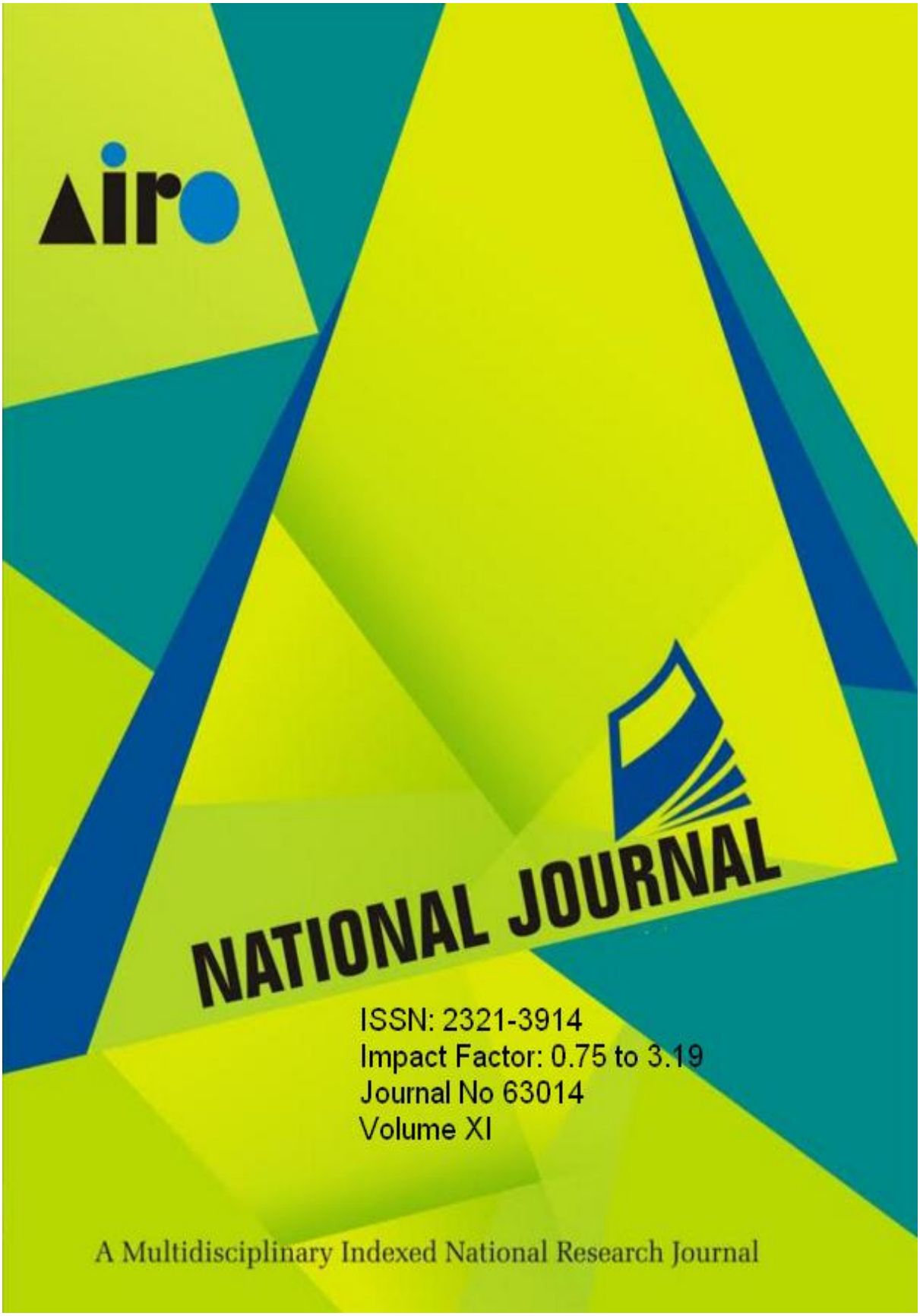
Airo
NATIONAL JOURNAL
ISSN: 2321-3914
Impact Factor: 0.75 to 3.19
Journal No 63014
Volume XI
A Multidisciplinary Indexed National Research Journal

Airo National Research Journal
Volume XI, ISSN: 2321-3914
August, 2017
Impact Factor 0.75 to 3.19
UGC Approval Number 63014

# ULTRAFAST MICROSCOPY: WITH THE ROLE OF FEMTO SECOND WITH OPTICS

**Rajeev Ranjan**

Research Scholar, (Deptt. of Mechanical Engineering), Kalinga University, Raipur

Supervisor: Dr. H. S. Suhas



## *ABSTRACT*

*The ultra-fast technology developed based on the generation and application of stabilized optical frequency comb lasers have been extremely successful in opening new time domains, the wavelength of light, and in particular diffraction, have limited the spatial resolution ofoptical microscopy to the limit of on the order of λ/2. Innovative techniques basedon super-resolution and near field optical microscopy have enabled the localization of bright molecular emitters beyond the diffraction limit down to a few nanometrescale.Through time dependent sampling they can follow the motion of single emitters, or theflow energy or charge by coherent or diffusive pathways in complex environments to energize the reporting emitters. the structural evolution of aluminium as it underwent an ultra-fast laser –induced solid-liquid phase transition. We used 600-femtosecond electron pulses of the liquid structure where only short-range atomic correlation where present; this transition occurred in 3.5picosecond for thin film aluminium with an excitation of 70 milli joules per square Centimetre. Pulse length is inversely proportional to the optical spectrum of the laser beam therefore ultra-short pulses have a very broad spectrum, e.g. the gain bandwidth of Ti-Sapphire is 128 THz thusthe shortest pulse duration is 3.4 femtoseconds (3.4 • 10-15 seconds). Technically, such pulses are no longer the shortest artificially generated electromagnetic waves, Otto second ($10^{-18}$ second) pulses have already been achieved but this technology is still far from commercial use. the femtosecond-laser-ablation technique provides a fast and cheaper alternative for the realization of materials with engineered optoelectronic properties for THz applications.*

***Keywords:*** *microscopy, femtosecond, optics*

## INTRODUCTION

Ultrafast phenomena are too fast to be directly monitored with electronics, optical techniques, such as pump-probe measurements, are required. With such techniques, phenomena occurring on time scales of picoseconds or femtoseconds can be monitored. Examples of such

phenomena are femtosecond dynamics of electrons (particularly in solids, e.g. in semiconductor devices such as SESAMs), light-induced phase changes (e.g. melting or vaporization of metals), chemical reactions, and processes in plasmas. Optical materials possess a specific quality, the phase velocity of light inside the material depends on the frequency (or wavelength), and equivalently the group velocity depends on the frequency. This is called chromatic dispersion or group-velocity dispersion (GVD). This means that for different wavelengths of light the refractive index inside of the material is different. Therefore, the group velocity at which light passes through the material is different for each wavelength. An ultrashort pulse is an electromagnetic pulse with a time duration of one picosecond ($10^{-12}$ second) or less. Since ultrashort phenomena are too fast to be directly measured with electronic devices such events are sometimes referred to as ultrafast

Currently, ultrafast optics is being extended into the sub-femtosecond region, where attosecond pulses (or pulse trains) are obtained, e.g. via high harmonic generation with intense ultra-short pulses.

Applications of ultrafast optics are:

• Ultrashort pulse generation;

• Maintaining of the temporal properties of the pulse;

• Stretched pulse compensation;

• Pulse stretching. Altechna offers products for each of these applications:

1. Ultrashort pulse generation:

a. Yb:KYW/KGW crystals

b. Ti:Sapphire crystals

2. Maintaining of the temporal properties of the pulse:

a. Low GDD mirrors

b. Ultrafast thin film polarizers

c. Watt Pilot - Motorized Attenuator, Ultrafast Version

d. Reflective beam expander

3. Stretched pulse compensation: a. Gires-Tournois Interferometer (GTI) mirrors

4. Pulse stretching: a. Brewster angle dispersing prisms

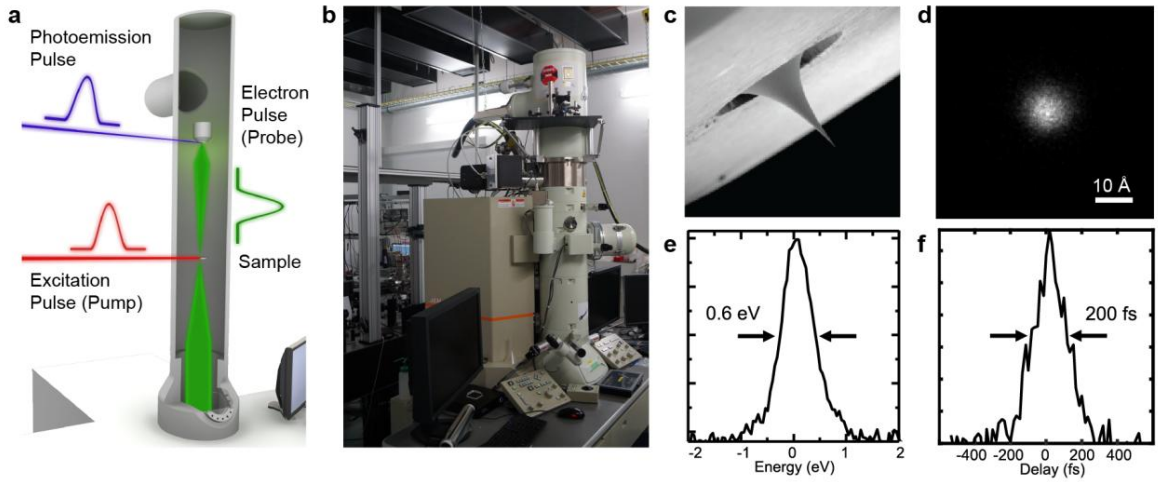


Laser which emits optical pulses with a duration well below 1 ps (→ *ultrashort pulses*), i.e., in the domain of femtoseconds (1 fs = $10^{-15}$ s). It thus also belongs to the category of ultrafast lasers or ultrashort pulse lasers. The generation of such short pulses is nearly always achieved with the technique of passive mode locking Some femtosecond lasers offer a stable linear polarization of the output, whereas others emit with an undefined polarization state.

High pulse repetition rates enable widely spaced stabilized optical frequencies that can be easily resolved and accessed so that individual optical frequencies can be selected and modulated.

The fundamentals of laser ablation process using ultrashort laser pulses are not still fully understood. Pulse duration of femtosecond laser pulse is shorter than electron-to-ion energy transfer time and heat conduction time in the sample lattice.

**REVIEW OF LITERATURES**

The aim of our investigations is to understand on which time scale do laser induced structural transitions occur, which relaxation channels are present and weather these relaxation channels be controlled by laser parameters like intensity, duration, and light frequency. An important question which we attempt to answer is if there are fundamental differences between laser-induced and thermally induced bond breaking and phase transitions. Important aspects considered in our theory are:

The admission of all relaxation channels in the response to an electron hole plasma, including the calculation for all degrees of freedom and the admission of changes in sample volume andgeometry.The, handling of the electronic non-equilibrium caused by strong laser excitation and its subsequent equilibration and relaxation. The treatment of laser pulses with finite durations $\geq 0$. Experimental Procedures Device fabrication methods Standard soft-lithography techniques, with some modifications were used to fabricate the two-layer microfluidic device described.

The bottom layer that transports the C elegans is here after termed the "flow layer," and the top layer that both immobilizes the worms and actuates the valve structures on the chip when pressurized will be referred to as the ‘‘control layer’’. Photoresist patterns, produced using Mylar masks (CAD/Art Services), were used to create the molds for all poly dimethyl siloxane (PDMS; Sylgard 184, Dow Corning Corp) microfluidic structures. To begin, we first pattern the sieve structures by spin coating SU-8 3005 onto a 4" silicon wafer to a thickness of 8–10 mm. The sieve structures are the arrays of short flow outlets located in the trapping, loading, and staging areas.We, then coated SU-8 2025 atop the sieve structures at a thickness of 30–35 mm and created the remainder of the flow layer mold by alignment and exposure through a second photomask using a mask aligner. The mold for the control layer was fabricated with combined patterns of a positive resist (AZ 50XT, Applied Electronic Materials) and a negative resist (SU-8 2025). Reflow of the positive resist at 125˚C for 4 min was performed to create semi-circular channel cross-sections. Opto-mechanical setup The, laser axotomy setup incorporates custom optics to deliver femtosecond laser pulses for surgery into a home-built epi-fluorescence microscope. We carried out axotomies using a train of femtosecond laser pulses at a center wavelength of 802 nm generated at a repetition rate of 1 kHz (Spitfire, Spectra Physics). The beam energy was measured with an energy meter prior to performing all axotomies and adjusted with two sets of half wave plates/cube beam-splitters pairs.

## RESEARCH METHODOLOGY

To selectively image the single Si NW without a background signal from directtransmission through the substrate, which is normally much bigger than the signal from the SiNW, an additional measurement step was necessary. This entailed recording the probe imageon a blank region of the sapphire substrate in the same manner. Furthermore, we obtained the spatial resolution of our UOWFMsystem (~770 nm) from measuring the cross section of the NW image.

Using this method, background-free microscopic images could be obtained, even for samples with transparent substrates. To obtain time-resolved optical images on the single Si NW, our UOWFM experiments were performed in the same manner as our experiments on the Au patterned amorphous Sifilm, i.e. the transmitted probe beam was directed to the 2D smart pixel detector, which allowed us to capture a time-dependent image of the single NW. We note that since the time-depend entimages were obtained while modulating the pump beam and detecting the probebeam, as in a standard pump-probe experiment, it is unnecessary to follow the proceduredescribed above to obtain static images of a sample on a transparent substrate (since there isno photoinduced change in the probe transmission through the substrate).

Images of the Si NW at different time delays between pump and probe, with both beamsoverlapped on the center of the NW. At $t$ = 0, a bright image wasobserved,

indicating that photoexcited carriers in the Si/SiO2 NW modify the probetransmission, followed by a decay in the image intensity, as seen for *t* = 100 ps. At*t* = 400 ps the brightness was much weaker, but still observable, which was due to the surfacepassivation provided by the SiO2 shell in un-passivated NWs the ΔT/T signalreturns to zero within ~200 ps. Finally, we note that since the pump and probe spotdiameters were much smaller than the length of the NW along its axis (~9 μm), only thecenter of the NW could be photoexcited and detected, which caused the brightest region ineach image to be circular. In general, optimization of this system will requirecareful consideration of the pump and probe beam profiles, both to obtain diffraction-limitedspatial resolution as well as to optimize the system for a given sample.

## RESULTS AND DISCUSSION

An objective lens with a high numerical aperture (NA51.4) tightly focused the laser beam to an estimated 1/e2 spot size of 620 nm. Automated microscopy was performed with a 56air objective and a 636 oil-immersion objective For fluorescence imaging of green fluorescence protein (GFP) labelled axons, a mercury arc lamp (XCite 120, EXFO) provided the excitation light source passing through a FITC filter set. A three-axis translation stage made of individual actuators (LTA-HS, Newport) and operated by a single controller (ESP301-3, Newport) positioned the samples. These stages could translate at up to 5 mm/s with a minimal incremental motion of 100 nm and a lateral resolution of 35 nm (achieved after backlash compensation). High precision positioning was performed by a three-axis piezoelectric actuator with a minimal theoretical step size of 25 nm and a travel range of ¡10 mm for each axis. A CCD camera (139261040 pixels with 6.45 mm pixel size, CoolSnap ES, captured the images with fields of view (FOV) of 1.861.34 mm2 at 56 magnification (1.29 mm/pixel, 1.88 mm resolution at 500 nm) and 1436107 mm2 at 636 magnification with 1.4 NA (102 nm/pixel, 214 nm resolution at 500 nm). For controlling the device flow layer, pressurized external fluid chambers controlled by three-way solenoid valves (Lee Company, LHDA0521111H, respectively) were coupled to the chip via a manifold (LFMX0510418). These chambers contained M9 buffer solution (22 mM KH2PO4, 22 mM Na2HPO4, 85 mM NaCl, 1 mM MgSO4, in dH2O). To minimize debris, all M9 buffer was passed through 1.2 mm in-line filters (Acrodisc, Pall Corp.) prior to entering the microfluidic device. Valves were independently actuated with a multichannel amplifier (Automate Scientific) that was controlled with a DAQ card (USB6501, National Instruments). All automation steps, including stage positioning, valve actuation, and image processing, were performed with a custom-written LabVIEW (National Instruments) program. An Automated Laser Nano-Axotomy Platform was maintained at 16.5˚C on NGMSR (Streptomycin-Resistant Nematode Growth Medium) agar plates seeded with HB101 E. coli bacterial culture using standard procedures. We studied the regeneration on one of the touch receptor neurons – the anterior

lateral microtubule (ALM). Depending on the orientation of the immobilized worm, the axotomy was performed on either left or right ALM neuron (ALML or ALMR). We used the strain SK4005: zdIs5 (Pmec-4:gfp) + lin- 15(+) I, which expresses GFP in the six touch receptor neurons. Populations of age-synchronized worms were prepared by collecting and isolating embryos following hypochlorite treatment. Developmental synchronization resulted in a low degree of variability in worm's body length which significantly improved identification rates of target neurons. Gravid adults were lysed with a small volume of a 2:1 mixture of sodium hypochlorite and 4 M sodium hydroxide, and the collected eggs were suspended in M9 buffer overnight on a rocker to aerate. The embryos hatched overnight and were arrested in the L1 stage until food was reintroduced. The L1 larvae were then placed on agar plates and allowed to grow for 48 hours, at which point the larvae had grown into worms at the young. Since light couples primarily with the electronic system, a laser pulse of moderate intensity produces the excitation of electrons from occupied to unoccupied levels. This creation of electron-hole pairs occurs with a time-dependent probability which is proportional to the (time-dependent) intensity of the laser field. As a consequence of the extremely fast excitation process, a non-equilibrium distribution of electrons is created. We describe laser induced structural changes with the help of molecular dynamics simulations (MD). This means, that we treat the nuclear degrees of freedom of the problem classically. However, the electron dynamics must be treated quantum mechanically. The forces acting on the atoms are obtained as and cause the lattice dynamics, described by Newton's equations of motion It is known that the laser excited material reacts by a very fast expansion, which will be stronger in areas that have absorbed more laser energy; the laser intensity distribution can be expected to be Gaussian in space [200]. Thus, a surface profile is possible after a few picoseconds. For this reason, one possible approach to describe the situation is to make the volume and shape of the MD super cell variable, depending on the forces that prevail within. On the other hand, the considered MD super cell will because of its small extensions be surrounded by material that is subject to approximately the same degree of excitation. Therefore, locally a translation invariance is existent that is the prerequisite for the use of periodic boundary conditions.

In the case of the potential energy surface U(frijg) is usually approximated by a model potential, like, for example, Lennard-Jones which consist of functions of the interatomic distances. For the description of laser induced structural changes, however, such model potentials are not useful, since they do not contain the electrons as degrees of freedom. Therefore, they do not allow any reasonable description of the excitation process. As mentioned at the beginning of this section, the laser pulse couples primarily with the electronic system. Hence, for the studies to be presented in this chapter, the many-body potential energy surface must be derived from a microscopic electronic Hamiltonian.

We assume that the valence electrons of the covalent solid can be described by an effective single-particle Hamiltonian in a restricted Hilbert spaces panned by M functions, depends of course, on the electronic degrees of freedom, but also on the interatomic distances, since the properties of the electrons change if r change.

The use of a "double optical pump" technique intera-hertztime-domain emission spectroscopy as an alternative method to investigate the lifetime of photo-excited carriers in semiconductors. Compared to the commonly employed optical pump-probe transient photo-reflectance, this non-contact and room temperature characterization technique allows relative ease in achieving optical alignment.

Using this "double optical pump" THz-TDES scheme, experiments were carried out at room temperature and in reflection geometry to measure the decay characteristics of the THz emission from LT-GaAs samples grown by MBE on semi-insulating GaAs substrates.

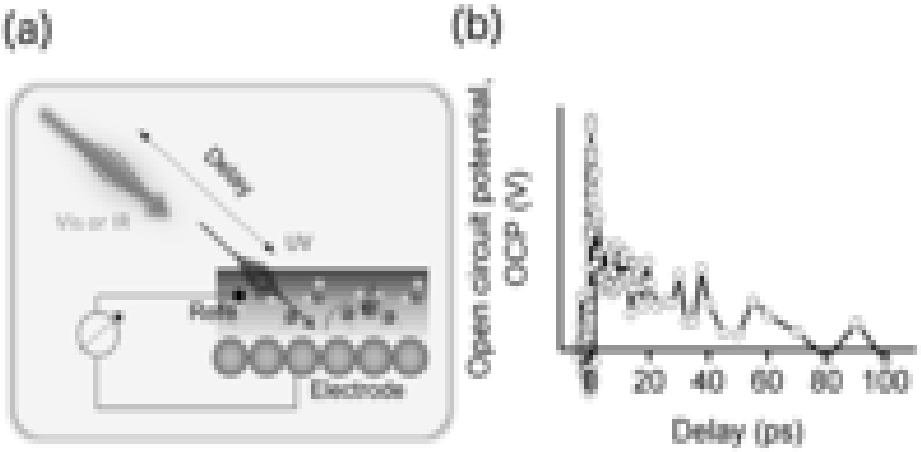


Figure: (a) Schematics of the double pump experiment. A pulse of UV light first arrive at the electrode and photo injects electrons into the electrolyte. After a controlled delay, a pulse of lower energy interacts resonantly with the excitation.

(b) Extracted decay of the open circuit potential for a 2nd pump pulse at 1.85 eV as a function of delay.

We have used ultrafast laser pulses in the ultraviolet (UV) range with the intent of triggering photo injection from a 200 nm thick polycrystalline gold electrode to the 0.5 M $Na_2SO_4$ electrolyte. To enable high-precision laser axotomies, we have previously established a new methodology of pressurizing and deforming a membrane to immo.The interaction of femtosecond laser pulses and solids gives rise to a large variety of novel and interesting effects. An important part of the laser induced ultrafast phenomena observed recently is concerned with structural changes. Laser pulses of

durations ranging from a few femtoseconds up to half a picoseconds and intensities above 1012 W/cm2 may induce lattice instabilities which lead to thermal and non-thermal structural changes bilize worms directly against the optical interface during surgery. By eliminating an extra layer of PDMS or dead channel volume between worms and the cover glass, our design offered ideal optical focusing and accuracy of ablation for studying the complete regeneration process. In our current design, adopting the same immobilization methodology we redesigned the chip into a unique configuration to enable its full automation. The An Automated Laser Nano-Axotomy includes five distinct parts-

(1) A loading chamber for housing a population of up to 250 worms,

(2) A staging area for isolating a single worm from the population in the loading chamber and delivering it to the trapping area,

(3) A trapping area designed to ensure repeatable and rapid immobilization of single worms near to the focused laser spot,

(4) 3D interconnects for enabling transition to completely sealing valves, and

(5) flush exit outlets for transitioning processed worms to an off-chip location.

In the following sections, we detail our design considerations and how each design specification contributed to fulfilling these considerations. We then explain the automation sequence that includes both automated actuation of valves and on-chip flow, as well as image analysis of captured worms and their neurons. The description of the custom-developed software and corresponding hardware list is given in File S1. This supplementary document also includes the instructions for the software download and installed.We, successfully combined efficient and accurate image analysis techniques with this microfluidic platform to perform multiple surgeries in a serial manner, with synchronized valve and flow progression facilitating rapid transport and immobilization of individual worms.

## CONCLUSION

We presented applications of our method to a variety of materials, focusingour attention on the microscopic processes underlying laser induced structural phase transformations. In diamond, we find that the dominant damage mechanism upon absorption of an energy of roughly 1eV/atom from an ultrashort laserpulse is a rapid graphitization. Within approximately 200 fs of the peak of an above-threshold pulse, the density of states of the material dramatically changesits character from that of diamond to that of graphite. In the study of the ablationof graphite we find a previously unknown damage mechanism that doesn’t involve the breaking of bonds in the graphite planes.Instead, strong vibrational excitation of the intact planes lead to inter-plane collisions and to the removal of entire planes through the transferral of momentum. This mechanism may berelevant in the interpretation of time dependent reflectivity measurements andfor understanding the formation of

carbon nanotubes. At higher deposited laserenergies we describe the nonequilibrium melting of graphite which leads to acarbon phase dominated by linear carbon chains before the material evaporates. This observation also holds for the other materials we have studied.The interaction of an intense laser pulse with a C60 molecular crystal under pressure leads to ultrafast destruction of the C60 molecules and the formation of a homogeneous carbon melt. Finally, in the laser fragmentation of a carbon nanotube we can distinguish two damage processes, namely the emission of carbon monomers and the unfolding of the tube after laser induced bondbreaking.In a study of the laser melting of a silicon film we show that the development ofthe pair correlation function of the liquid state takes less than 200 fs, confirmingthat the laser induced electron hole plasma leads to a non-thermal melting.

## REFERENCES

**[1]** Bennemann KH (2009) Ultra-fast dynamics in solids: non-equilibrium behaviour of magnetism and atomic structure. Ann Phys 18:480–560.

[2] Tom HWK, Aumiller GD, Brito-Cruz CH (1988) Time-resolved study of laser-induced disorder of Si surfaces. Phys Rev Lett 60:1438–1441.

[3] Harb M, et al. (2008) Electronically driven structure changes of Si captured by femtosecond electron diffraction. Phys Rev Lett 100:155504.

[4] Saeta P, Wang JK, Siegal Y, Bloembergen N, Mazur E (1991) Ultrafast electronic disordering during femtosecond laser melting of GaAs. Phys Rev Lett 67:1023–1026.

[5] Kim AMT, Callan JP, Roeser CAD, Mazur E (2002) Ultrafast dynamics and phase changes in crystalline and amorphous GaAs. Phys Rev B Condens Matter Mater Phys 66:245203.

[6] Chen P, Tomov IV, Rentzepis PM (1996) Time resolved heat propagation in a gold crystal by means of picosecond X-ray diffraction. J Chem Phys 104:10001–10007.

[7] Hartland GV, Hu M, Sader JE (2003) Softening of the symmetric breathing mode in gold particles by laser-induced heating. J Phys Chem B 107:7472–7478.